Synthesis and cytotoxicity studies of Cu(I) and Ag(I) complexes based on sterically hindered β -diketonates with different degrees of fluorination

Maura Pellei,^{a,*} Jo' Del Gobbo,^a Miriam Caviglia,^a Deepika V. Karade,^b Valentina Gandin,^c Cristina Marzano,^{c,*} Anurag Noonikara Poyil,^b H. V. Rasika Dias,^{b,*} Carlo Santini^a

^aSchool of Science and Technology, Chemistry Division, University of Camerino, Via Madonna delle Carceri (ChIP), 62032 Camerino, Macerata, Italy

^bDepartment of Chemistry and Biochemistry, The University of Texas at Arlington, Box 19065, Arlington, Texas 76019-0065, United States

^cDepartment of Pharmaceutical and Pharmacological Sciences, University of Padova, via Marzolo 5, 35131 Padova, Italy

*Corresponding authors:

maura.pellei@unicam.it (M.P.); dias@uta.edu (H.V.R.D.); cristina.marzano@unipd.it (C.M.)

KEYWORDS. Copper(I); Silver(I); Phosphanes; Cytotoxicity; Spectroscopy; X-ray

Abstract

Design, synthesis, and *in vitro* antitumor properties of Cu(I) and Ag(I) phosphane complexes supported by the anions of sterically hindered β-diketone ligands, 1,3-dimesitylpropane-1,3-dione (HL^{Mes}), and 1,3-bis(3,5-bis(trifluoromethyl)phenyl)-3-hydroxyprop-2-en-1-one (HL^{CF3}) featuring trifluoromethyl or methyl groups on the phenyl moieties have been reported. In order to compare the biological effects of substituents on the phenyl moieties, the analogous copper(I) and silver(I) complexes of the anion of the parent 1,3-diphenylpropane-1,3-dione (HL^{Ph}) ligand were also synthesized and included in the study. In the syntheses of the Cu(I) and Ag(I) complexes, the phosphane coligands triphenylphosphine (PPh₃) and 1,3,5-triaza-7-phosphaadamantane (PTA) were used to stabilize silver and copper in +1 oxidation state, preventing the metal ion reduction to Ag(0) or oxidation to Cu(II), respectively. X-ray crystal structures of HL^{CF3} and the metal adducts [Cu(L^{CF3})(PPh₃)₂] and [Ag(L^{Ph})(PPh₃)₂] are also presented. The antitumor properties of both classes of metal complexes were evaluated against a series of human tumor cell lines derived from different solid tumors, by means of

both 2D and 3D cell viability studies. They display noteworthy antitumor properties and are more potent than cisplatin in inhibiting cancer cell growth.

Introduction

Medicinal inorganic chemistry offers possibilities for the design of therapeutic agents not readily available to organic compounds. 1, 2 Currently, many chelating ligands and delivery systems for metal-based drugs have been developed to obtain more potent, clinically effective, and less toxic metal-based antiproliferative drugs with improved selectivity towards tumour cells.^{3, 4} Group 11 metal complexes showed encouraging perspectives in this regard and several noble metal complexes were investigated for their antitumoral properties.⁵⁻⁷ β-Diketones compounds represent a very important class of reagents in the synthesis of heterocyclic compounds. 8 The β-diketone scaffold is not very common in nature though it is the main feature of curcumin and its derivatives. 9 Although β-diketones represent one of the oldest classes of chelating ligands, 10, 11 their coordination chemistry continues to attract much interest, due to the ability of related metal complexes to support several unique and important catalytic reactions. 12 It is often noted that even modestly sterically hindered βdiketones offer improvements over the parent acetylacetone. ¹³ Truly hindered β-diketones only recently have been made synthetically accessible. 14 The presence of steric bulk on βdiketones is of high interest for their peculiar coordination behavior useful to improve their catalytic activity and selectivity. 15, 16 β-diketonates have been used as supporting ligands for Ti(IV), 17, 18 Ru(II), 19-25 Rh(I), 26, 27 Pd(II) and Pt-based anticancer agents. 29-33 They have also been reported to induce apoptosis in human tumor cells.³⁴ In an early investigation, several platinum(II) complexes with β-diketonate ligands as leaving groups were studied, revealing that the ligands play an integral role in modulating toxic side effects.³⁵ In particular, the phenyl ring substituents increase the lipophilicity and improve cellular uptake of the resulting complexes, whereas the electron-withdrawing CF₃ groups increases the hydrolysis rates of the complexes in aqueous solution.

Despite the enormous amount of work devoted to synthesis and characterization of copper(II) β -diketonate complexes, ³⁶ there are relatively few reports devoted to the corresponding Cu(I) complexes perhaps due to their tendency to undergo disproportionation to copper metal and copper(II) compounds in the absence of stabilizing ligands. ^{37, 38} Reports of triorganophosphane adducts, (β -diketonate)Cu(PR₃)_n, are also relatively scarce. ³⁹⁻⁵²

Several silver(I) β -diketonates have been synthesized and structurally characterized. ⁵³⁻⁵⁷ In particular, fluorinated β -diketonate ligands were used to construct coordination polymers, ⁵⁸⁻⁶⁰ stabilize multinuclear ethynide or thiolate clusters, ^{61, 62} and as precursors for chemical vapor deposition processes. ⁶³ Moreover, photosensitivity of silver β -diketonates makes it possible to obtain functional materials even at room temperature. ^{64, 65} However, very little attention has been paid to the study of phosphanes adducts of silver(I) β -diketonates, ^{40, 66-71} although they may also display a rich structural diversity.

To our knowledge, with the exception of Cu(II) derivatives of curcumine, 72,73 Casiopeinas®like compounds (Cas III)74-77 and analogous mixed 1,10-phenanthroline and 4,4,4-trifluoro-1-phenyl-1,3-butanedionate,⁷⁸ 2,2-bipyridine 4,4,4-trifluoro-1-(2-furyl)-1,3and benzoylacetonate,81 butanedionate^{79,} acetylacetonate⁸² thenoyltrifluoroacetonate,83 very few studies on the anticancer activity of group 11 metal complexes of β-diketones have been reported in the literature to date.⁸⁴ Copper(I)- and silver(I)-based anticancer complexes supported by β-diketonate ligands remain an unexplored research field. Therefore, as part of our continuous investigation on the chemical and biological properties of copper- and silver-containing coordination compounds, 85-91 we report here for the first-time a study on the syntheses, characterization and biological evaluation of new Ag(I) and Cu(I) complexes containing phosphanes and the anion of the β-diketone ligands, 1,3-dimesitylpropane-1,3-dione (HL^{Mes}), 1,3-bis(3,5bis(trifluoromethyl)phenyl)-3-hydroxyprop-2-en-1-one (HL^{CF3}) and 1,3-diphenylpropane-1,3dione (HLPh). The ligands were selected to systematically modify the electronic properties and hydrophobicity of the resulting metal complexes using phenyl, mesityl and trifluoromethyl-phenyl groups, respectively. On the other hand, fluorine-containing compounds are of relevant interest in modern medicinal chemistry and, in general, they are of special interest for use in drug design because of the good biological activity and low toxicity of molecules containing the trifluoromethyl moieties. 92-94 Selective introduction of fluorine into a therapeutic or diagnostic small molecule candidate can enhance/modulate a number of physicochemical and pharmacokinetic properties such as improved metabolic stability and enhanced membrane permeation. 95 Indeed, the substitution of a main group by a trifluoromethyl group in a molecule might be expected to induce great changes in molecular properties, in terms of hydrophobicity, solubility and electronegativity affecting not only metabolic stability but also binding affinities toward target proteins. 96-99 In designing the novel β-diketonates metal complexes, the lipophilic triphenylphosphine (PPh₃) and hydrophilic 1,3,5-triaza-7-phosphaadamantane (PTA) were selected as co-ligands, in order

to stabilize copper and silver in their +1 oxidation state and to confer different solubility properties to the corresponding metal complexes.

Search of Cambridge Structural Database¹⁰⁰ reveals that many of the structurally well-authenticated phosphane adducts of copper(I) and silver(I) involve fluoroalkyl substituted β -diketonates. Among these, copper adducts are relatively more common, and often feature two-phosphane ligands bonded to copper producing tetrahedral molecules. Relatively larger number of reported silver-complexes are three-coordinate with one phosphane on silver(I). Two representative examples are depicted as \mathbf{A}^{52} and \mathbf{B}^{71} in Figure 1.

Figure 1. Several examples of structurally authenticated copper(I) and silver(I) phosphane complexes.

Notably, structural data on copper and silver phosphane complexes supported by diaryl βdiketonates are quite limited. They include (1,3-diferrocenylpropane-1,3- $1),^{50}$ (1,3-diphenyl-1,3dionato)bis(triphenylphosphine)copper(I) (C, Figure $1)^{51}$ dionato)bis(triphenylphosphine)copper(I) (**D**, **Figure** and (1,3-diphenyl-1,3dionato)trimethylphosphine)copper(I) (E, Figure 1).41 In this paper, we report X-ray crystal structures of [Cu(L^{CF3})(PPh₃)₂] and [Ag(L^{Ph})(PPh₃)₂]] as two new additions to this group. Finally, the in vitro antitumor properties of the new Cu(I) and Ag(I) complexes as well as of the corresponding uncoordinated ligands were evaluated against several human cancer cell lines derived from different solid tumors by means of both 2D and 3D cell viability tests. The cytotoxic data have been compared with those obtained with cisplatin, the reference metalbased chemotherapeutic drug.

Results and discussion

Synthesis and characterization

The β -diketones 1,3-bis(3,5-bis(trifluoromethyl)phenyl)propane-1,3-dione (HL^{CF3})¹⁰¹ and 1,3-dimesityl-propane-1,3-dione (HL^{Mes})¹⁰² were prepared according to literature procedures and fully characterized by several methods. The X-ray crystal structure of HL^{CF3} is presented in the Supporting Information (Figure S1). The 1,3-diphenylpropane-1,3-dione (HL^{Ph}) was obtained from commercial sources and used as received. β -Diketones are capable of ketoenol tautomerism, and the tautomers exist in equilibrium with each other in solution; although, in most organic solvents, β -diketones are predominately enolized. ¹⁰³ The sodium salts of β -diketonate ligand NaL^{CF3} (1), NaL^{Mes} (2) and NaL^{Ph} (3) were prepared, using a modified literature method of analogous sodium β -diketonates, ¹⁰⁴ from the reaction of HL^{CF3}, HL^{Mes} and HL^{Ph} respectively, with NaOH in ethanol solution, and isolated as orange whitish solids in 85% yield for NaL^{CF3}, in 74% yield for NaL^{Mes} and in 80% yield for NaL^{Ph} (Scheme 1).

Scheme 1. Synthesis of compounds **1-11**.

Compounds **1**, **2** and **3** were fully characterized by multinuclear NMR spectroscopy, FT-IR, ESI-MS and elemental analysis. The two (CF₃)₂Ph, mesityl and phenyl groups are magnetically equivalent in the 1 H and 13 C NMR. The 1 H-NMR spectrum of **1**, recorded in DMSO-d₆ solution, shows a single set of resonances for the two CH protons in *ortho-* and in *para-*positions of aromatic rings at 8.48 and 8.08 ppm, respectively, while the signal at δ 6.57 ppm is assignable to the COCHCO proton of the diketone. 19 F NMR spectrum of **1** displayed a singlet at δ -61.21 ppm. Analogously, the 1 H NMR spectrum of compound **2** in CDCl₃ includes single peaks assignable to (CH₃)₃Ph protons (δ 2.23, 2.24 and 6.72 ppm) and to the COCHCO proton of the diketone (δ 5.31 ppm), while in the spectrum of **3** recorded in acetone-d₆ the aromatic protons are at 7.46-8.07 ppm and the COCHCO proton of the diketone is at δ 6.87 ppm. Deprotonation of the β -diketonate ligands leads to a slight shift of the COCHCO group resonance with respect the protonate species (δ 6.89 ppm for HL^{CF3},

5.77 ppm for HL^{Mes} and 6.89 for HL^{Ph}, in CDCl₃). The infrared (FT-IR) spectra of β -diketones generally exhibit very strong bands in the 1200-1650 cm⁻¹ region. For compounds **1**-3, the bands in the range 1565-1643 cm⁻¹ are assigned to the ν (C=O) stretching modes. For compound **1** the bands at 1163-1164 and 1110-1121 cm⁻¹ can be assigned to the C-F stretching and CF₃ deformation, respectively.

For derivatives of HL^{CF3} ligand, the Cu(I) complex [Cu(L^{CF3})(PPh₃)₂] (4) was prepared from the reaction of PPh₃, Cu(CH₃CN)₄PF₆ and the sodium salt NaL^{CF3}, while the Ag(I) complex [Ag(L^{CF3})(PPh₃)₂] (**5**) was prepared from the reaction of PPh₃, AgNO₃ and the sodium salt NaL^{CF3} (Scheme 1). The IR spectra carried out on a solid sample of 4 and 5 show all the expected bands for the β-diketone ligand and the triphenylphosphine co-ligands. The absorptions due to the C=O stretching are at 1582-1626 cm⁻¹, while bands due to C-F stretching and CF₃ deformation are at 1169-1171 and 1125-1126 cm⁻¹, respectively. They don't significantly vary with respect to the same absorptions of the carbonyl group detectable in the spectrum of the free ligand salt 1. The ¹H-NMR spectra of complexes 4 and 5, recorded in CDCl₃ solution at room temperature, show a single set of resonances for the β-diketone moiety, indicating that the protons of the aromatic rings are equivalents, with a slight shift due to the coordination to the metal centre. The PPh₃ co-ligands show a characteristic series of peaks in the range 7.22-7.44 ppm. ¹⁹F NMR spectra of **4** and **5** in CDCl₃ displayed singlets at δ -62.64 and -62.66 ppm, respectively. The ESI-MS study was performed by dissolving 4 and **5** in CH₃CN and recording the spectra in positive- and negative-ion mode. The structure of 4 and 5 was confirmed by the presence of peaks attributable to the [Cu(PPh₃) + CH₃CN]⁺, [Cu(PPh₃)₂]⁺, [Ag(PPh₃) + CH₃CN]⁺ and [Ag(PPh₃)₂]⁺ species, being positive fragments of the dissociation of the ligand from the complex. In addition, in the negative-ion mode spectra we observe peaks at 495 due to the [LCF3] fragment.

The Cu(I) complexes of HL^{Mes} and HL^{Ph} ligands, [Cu(L^{Mes})(PPh₃)₂] (**6**) and [Cu(L^{Ph})(PPh₃)₂] (**9**), were prepared from the reaction of PPh₃, Cu(CH₃CN)₄PF₆ and NaL^{Mes} (**2**) and NaL^{Ph} (**3**), respectively (Scheme 1). Analogously, the Ag(I) complexes [Ag(L^{Mes})(PPh₃)₂] (**7**) and [Ag(L^{Ph})(PPh₃)₂] (**10**) were prepared from the reaction of PPh₃, AgNO₃ and the sodium salts **2** and **3**, respectively (Scheme 1). The IR spectra carried out on a solid sample of **6**, **7**, **9** and **10** show all the expected bands for the β-diketone ligand and the triphenylphosphine co-ligands. The absorptions due to the C=O stretching are at 1548-1651 cm⁻¹ and they don't significantly vary with respect to the same absorptions in the spectra of the free ligand salts **2** and **3**. The ¹H-NMR spectra of complexes **6**, **7**, **9** and **10**, recorded in CDCl₃ or CD₃OD solution at room temperature, show a single set of resonances for the β-diketone moiety,

indicating that the protons of the aromatic rings are equivalents, with a slight shift due to the coordination to the metal center. The PPh₃ co-ligands show a characteristic series of peaks in the range 7.21-7.50 ppm. The ESI-MS study was performed by dissolving **6**, **7**, **9** and **10** in CH₂Cl₂/CH₃CN, CH₃OH or CH₃CN. In the positive-ion mode spectra we observed the presence of peaks attributable to the [Cu(PPh₃)₂]⁺ and [Ag(PPh₃)₂]⁺ species, being positive fragments of the dissociation of the ligand from the complexes. In addition, in the negative-ion mode spectra we observed peaks at *m/z* 307 and 223, due to the [L^{Mes}]⁻ and [L^{Ph}]⁻ fragments, respectively.

The Ag(I) complexes of HL^{Mes} and HL^{Ph} ligands, [Ag(L^{Mes})(PTA)] (8) and [Ag(L^{Ph})(PTA)]·H₂O (11), were prepared from the reaction of PTA, AgNO₃ and the sodium salts 2 and 3, respectively (Scheme 1). Several attempts to synthesize Ag(I) complexes with two PTA as coligands have been unsuccessful, even modifying the reaction conditions and stoichiometric ratio between the reagents. Analytical and spectroscopic data suggest the 1:1:1 stoichiometry for complexes 8 and 11, with PTA coordinated via phosphorus atom. On the other hand, PTA acts as a monodentate P-donor ligand in the vast majority of known complexes,¹⁰⁹ although in absence of crystallographic data we cannot exclude that the PTA binds the metal in bridging *N*,*P*-coordination mode.¹¹⁰

The IR spectra carried out on a solid sample of **8** and **11** show all the expected bands for the β -diketone ligand and the 1,3,5-triazaphosphaadamantane co-ligands. The absorptions due to the C=O stretching are at 1513-1610 cm⁻¹ and they don't significantly vary with respect to the same absorptions in the spectra of the free ligand salts. The ¹H-NMR spectra of complexes **8** and **11**, recorded in CD₃OD solution at room temperature, show a single set of resonances for the β -diketone moiety, indicating that the protons of the aromatic rings are equivalents, with a slight shift due to the coordination to the metal center. The PTA coligands show a characteristic series of peaks in the range 4.15-4.67 ppm, with an integration that confirms the 1:1 stoichiometry. The ESI-MS study was performed by dissolving **8** and **11** in CH₃OH. In the positive-ion mode spectra we observed at m/z 158 and 420 the presence of peaks attributable to the [PTA + H]⁺ and [Ag(PTA)₂]⁺ species, respectively, due to the dissociation of the ligand from the complexes.

It's interesting to note that the diagnostic COC*H*CO signal is at 6.17 and 6.21 ppm in the spectra recorded in CDCl₃ of [Cu(L^{CF3})(PPh₃)₂] (**4**) and [Ag(L^{CF3})(PPh₃)₂] (**5**) respectively, and the related peak is present at 6.57 ppm in the spectrum of the sodium salt NaL^{CF3} (**1**) in DMSO-d₆ solution and at 6.91 in the spectrum of HL^{CF3} in CDCl₃ solution. In the ¹³C{¹H}-NMR spectra of **4** and **5** the COCHCO signals are at 92.02 and 92.35 ppm, respectively,

and the related peak is at 90.91 and 93.82 ppm in the spectra of the free ligands **1** and HL^{CF3}. In the ¹H-NMR spectra of [Cu(L^{Mes})(PPh₃)₂] (**6**), [Ag(L^{Mes})(PPh₃)₂] (**7**) and [Ag(L^{Mes})(PTA)] (**8**), recorded in CDCl₃ or DMSO-d₆, the COC*H*CO signals are at 4.81-5.34, and the related peak is present at 5.29 and 5.77 ppm in the spectra of NaL^{Mes} (**2**) and HL^{Mes}, respectively, in CDCl₃ solution. In the ¹³C{¹H}-NMR spectra of **6-8** the COCHCO signals are at 101.66-103.75, and the related peak is at 103.85 and 105.48 ppm, in the spectra of the free ligands **2** and HL^{Mes}. Finally, the COCHCO signals are at 6.40-6.78 in the spectra recorded in CDCl₃ or CD₃OD of [Cu(L^{Ph})(PPh₃)₂] (**9**), [Ag(L^{Ph})(PPh₃)₂] (**10**) and [Ag(L^{Ph})(PTA)]·H₂O (**11**), respectively, and the related peak is present at 6.87 and 6.89 ppm in the spectra of the sodium salt NaL^{Ph} (**3**) and HL^{Ph} in acetone-d₆ and CDCl₃ solution, respectively. In the ¹³C{¹H}-NMR spectra of **9-11** the COCHCO signals are at 90.35-93.38 and the related peak is at 93.21 in the spectrum of the free ligand **3**. In the ¹³C{¹H}-NMR spectra of **9-11** the COCHCO signals are at 90.35-93.38, and the related peak is at 93.21 and 93.18 ppm, in the spectra of the free ligands **3** and HL^{Ph}.

The room temperature ³¹P{H}-NMR spectra of the Cu(I) complexes **4**, **6** and **9**, recorded in CDCl₃ or CD₂Cl₂ solution, gave single signals at -3.68, -5.41 and -3.96 ppm, respectively, downfield shifted with respect to the value of the free triphenylphosphine PPh₃ ($\delta = -4.85$ ppm in CDCl₃ and -5.55 ppm in CD₂Cl₂). The room temperature ³¹P{H}-NMR spectra of the Ag(I) complexes, recorded in CDCl₃ solution (compounds 5, 7, and 10) or CD₃OD solution (compound 8 and 11), gave singlet signals downfield shifted with respect to the value of the free phosphanes PPh₃ and PTA ($\delta = -4.85$ and -102.07 ppm, respectively). At 223 K, the spectra of 5 and 7 (in CDCl₃ solvent) show one pair of doublets in which the coupling of ³¹P to the ¹⁰⁷Ag and ¹⁰⁹Ag is resolved, in accordance with a stopped or slow triphenylphosphane exchange process: the ${}^{1}J({}^{107}Ag - {}^{31}P)$ and ${}^{1}J({}^{109}Ag - {}^{31}P)$ coupling constants are respectively in the range 408-430 and 472-496 Hz for compounds 5 and 7, being of the same order of magnitude of those reported for analogous silver(I) bis(triphenylphosphine) species. 111-113 At 223 K, compound **10** exhibits a broad doublet with a ¹*J*(Ag-³¹P) coupling constant of 439 Hz. The ratio of ${}^{1}J({}^{109}\text{Ag}-{}^{31}\text{P})/{}^{1}J({}^{107}\text{Ag}-{}^{31}\text{P})$ is in good agreement with the ${}^{107}\text{Ag}/{}^{109}\text{Ag}$ gyromagnetic ratio of 1.15. The room temperature ³¹P{H}-NMR spectra of complexes **8** and 11 with PTA coligands, recorded in CD₃OD solution, gave singlets centered at δ -83.73 and -83.82 ppm, while at 243 K they exhibit broad signals, centered at about -81 ppm, in which the coupling of ³¹P to ^{107/109}Ag is not resolved.

Compounds [Cu(L^{CF3})(PPh₃)₂] (**4**) and [Ag(L^{Ph})(PPh₃)₂] (**10**) produced crystalline material suitable for X-ray crystallography. They crystallize as discrete molecules in the space groups

P-1 and P2₁/n, respectively and the molecular structures are illustrated in Figures 2 and 3. There are two chemically similar molecules in the asymmetric unit of [Cu(L^{CF3})(PPh₃)₂]. Both the copper and silver complexes adopt distorted tetrahedral geometry. Complete details of the bond distances and angles are given in the Supporting Information. Although the diketonate based CuO₂C₃ metallacycle is essentially planar in [Cu(L^{CF3})(PPh₃)₂] (Figure 2), the AgO₂C₃ core of the silver complex [Ag(LPh)(PPh₃)₂] (Figure 3) adopts a half-boat conformation with the silver atom residing out O₂C₃ plane. The average Cu-P distance and Cu-O distances of [Cu(L^{CF3})(PPh₃)₂] (2.2256 and 2.071 Å, respectively) are shorter than the Ag-P and Ag-O distances in [Ag(LPh)(PPh₃)₂] (average 2.424 and 2.343 Å, respectively), which is expected due to the larger covalent radius of silver relative to copper. The P-M-P angles (M = Cu, Ag) are very similar between the two systems (128.50° and 129.20° for 4 and 10, respectively). A comparison of Cu-O distances of [Cu(LCF3)(PPh3)2] (av. 2.071 Å), to [Cu(LPh)(PPh₃)₂] (av. 2.058 Å) indicates that the latter featuring more electron donating βdiketonate has slightly shorter Cu-O contacts.⁵¹ The Cu-P distances of these two molecules (av. 2.2256 Å of [Cu(L^{CF3})(PPh₃)₂] and av. 2.250 Å of [Cu(L^{Ph})(PPh₃)₂]) show the opposite trend. We have also confirmed the identity of [Cu(L^{Mes})(PPh₃)₂] (6) using X-ray crystallography. It is also a four-coordinate, pseudo-tetrahedral complex (see Supporting Information, Figure S2). Unfortunately, weakly diffracting sample and crystal twinning of [Cu(LMes)(PPh3)2] prevented us from obtaining high quality data suitable for detailed analysis of structural features.

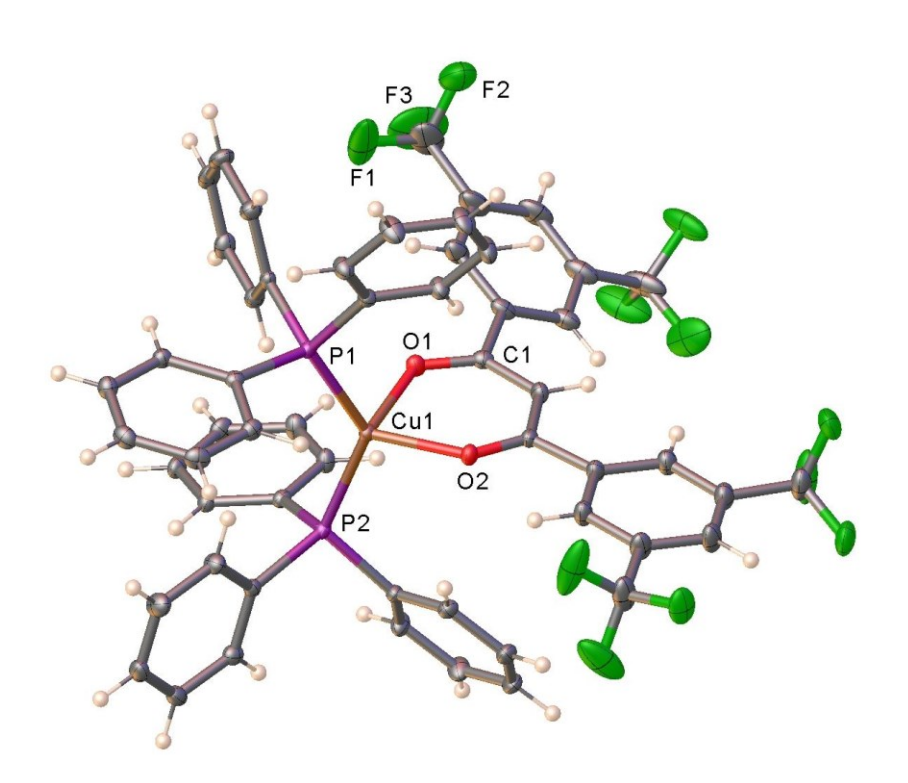


Figure 2. Molecular structure of [Cu(L^{CF3})(PPh₃)₂] **(4)** (only one of the two molecules present in the asymmetric unit is shown).

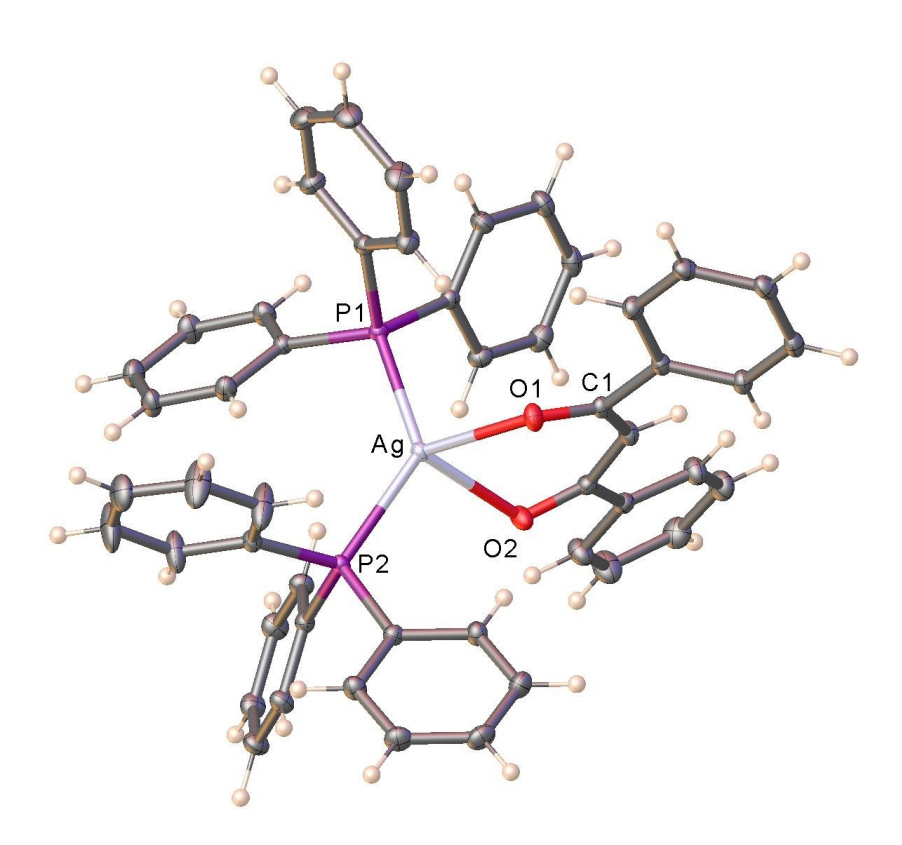


Figure 3. Molecular structure of [Ag(LPh)(PPh3)2] (10).

Biological studies

The stability of the new complexes in 0.5% DMSO/physiological solution was evaluated by UV-Vis spectroscopy. Spectra were collected every 24 h in the range of 240-640 nm over 72 h. The collected spectra for all complexes are reported in the Supporting Information, Figure S3) showing that all compounds were sufficiently stable under physiological conditions. All the spectra, and in particular the spectra registered for complexes **4** and **10** showed curves with a progressive increase in the baseline adsorption, probably due to solubility issues.

The Ag(I) and Cu(I) complexes and the corresponding uncoordinated ligands and their salts were evaluated for their cytotoxic activity towards various human cancer cell lines representative of different solid tumors. In particular, the in-house cancer cell panel contained examples of human colon (HCT-15), pancreatic (PSN-1 and BxPC3), testis (NTERA-2), and breast (MDA-MB-231) as well as of SCLC (U1285) and NSCLC (A549).

The cytotoxicity parameters, expressed in terms of IC_{50} obtained after 72 h of exposure to the MTT assay, are reported in Table 1. For comparison reasons, the cytotoxicity of the reference metal-based chemotherapeutic drug cisplatin was assessed in the same experimental conditions.

NaL^{Ph}/HL^{Ph} and NaL^{CF3}/HL^{CF3} ligands proved to be hardly effective against all tested cancer cell lines. On the contrary, NaLMes/HLMes ligands were quite effective in inhibiting cancer cell growth, with IC₅₀ values in the low micromolar range; however, the metal coordination significantly improved the potency compared to free ligand. It is interesting to notice that in the case of PPh₃-containing Cu(I) and Ag(I) complexes, metal coordination significantly improved the cytotoxic potency compared to free ligand, conversely, with [Ag(LMes)(PTA)] sensibly higher IC₅₀ values were always obtained, confirming that the bioactivity of the metal complex depends on the full set of coordinating ligands. All tested complexes demonstrated a marked cytotoxic activity towards cancer cell lines belonging to the in-house cancer cell panel, showing IC₅₀ values in the low/sub micromolar range. On average, the PPh₃ derivatives were more effective than cisplatin, whereas the two Ag(I) complexes bearing the PTA moiety were less effective than the reference metallodrug cisplatin. Among PPh₃ derivatives, Cu and Ag complexes bearing the L^{Mes} ligand were the most effective derivatives, with average IC₅₀ values of 2.4 and 4.0 µM, respectively. It is noteworthy that, against testis carcinoma NTERA-2 cells, [Cu(LMes)(PPh3)2] was up to 16-fold more efficacious than cisplatin in decreasing cell proliferation. Conversely, the weakest PPh3 derivatives were those bearing the L^{Ph} ligand. Interestingly, Cu(I) complexes containing the L^{CF3} and L^{Mes} ligands were much more effective (about 2-fold) than the corresponding Ag(I) derivatives whereas in the case of LPh ligand, the Ag(I) complex was about 2.7 times more effective than the corresponding copper derivative.

The *in vitro* antitumor activity of the newly developed Cu(I) and Ag(I) derivatives was also assayed in 3D cell culture models of human colon cancer cells. Although the two-dimensional cell cultures are the most employed assays for *in vitro* screening (due to the low cost, simplicity, and reliability), 2D methods are unable to mimic the *in vivo* properties of solid tumor models. On the other hand, 3D cell cultures are much more effective in closely mimicking the heterogeneity and complexity of the tumor mass, and therefore are more predictive for *in vivo* results than conventional 2D cell cultures. On these bases, we tested the activity of the newly developed complexes on spheroids obtained from human HCT-15 tumor cells. HCT15 cells are known for their ability to form spheroids, which makes them a valuable tool for studying the interactions between cancer cells and the surrounding

microenvironment. Human colon cancer cell spheroids were treated with the investigated compounds for 72 h, and cell viability was assessed by means of the acid phosphatase (APH) assay and the results are reported in Table 2. Results, reported in Table 2, were completely different from those obtained in 2D screenings, and clearly showed that among the new Cu(I) and Ag(I) complexes, only derivative [Cu(L^{CF3})(PPh₃)₂] possessed an antiproliferative activity against 3D tumor spheroids comparable to that of the reference drug cisplatin.

Table 1. 2D cytotoxicity.

| IC ₅₀ (μM) ± S.D. | | | | | | | | |
|--|------------|------------|------------|------------|------------|------------|------------|--|
| | NTERA-2 | HCT-15 | BxPC3 | U-1285 | PSN-1 | A549 | MDA-MB-231 | |
| HL ^{CF3} | 21.1 ± 0.9 | 43.5 ± 8.2 | >50 | 44.8 ± 5.8 | >50 | >50 | >50 | |
| NaL ^{CF3} | ND | |
| [Cu(L ^{CF3})(PPh ₃) ₂] | 1.3 ± 0.4 | 2.0 ± 0.5 | 1.2 ± 0.4 | 1.5 ± 0.5 | 4.4 ± 0.3 | 5.4 ± 0.9 | 5.3 ± 1.2 | |
| [Ag(L ^{CF3})(PPh ₃) ₂] | 3.5 ± 0.6 | 2.1 ± 0.4 | 2.9 ± 0.1 | 2.6 ± 0.2 | 6.3 ± 1.2 | 11.1 ± 1.5 | 11.3 ± 2.2 | |
| HL ^{Mes} | 3.6 ± 0.1 | 5.3 ± 0.7 | 7.5 ± 1.2 | 8.1 ± 1.1 | 5.2 ± 0.8 | 12.5 ± 3.6 | ND | |
| NaL ^{Mes} | 5.7 ± 0.8 | 4.6 ± 1.4 | 4.3 ± 0.9 | 5.1 ± 0.5 | 4.1 ± 0.3 | 9.1 ± 2.3 | ND | |
| [Cu(L ^{Mes})(PPh ₃) ₂] | 0.9 ± 0.3 | 1.2 ± 0.5 | 1.1 ± 0.4 | 1.2 ± 0.7 | 1.3 ± 0.5 | 5.6 ± 1.1 | 5.5 ± 0.8 | |
| [Ag(L ^{Mes})(PPh ₃) ₂] | 1.7 ± 0.6 | 2.5 ± 1.0 | 1.7 ± 0.5 | 2.7 ± 0.9 | 2.1 ±0.7 | 7.6 ± 1.4 | 9.5 ± 2.3 | |
| [Ag(L ^{Mes})(PTA)] | 12.8± 2.5 | 19.5 ± 3.1 | 14.9 ± 2.2 | 17.3 ± 2.7 | 15.7 ± 1.9 | 22.8 ± 3.3 | 28.1 ± 3.4 | |
| HL ^{Ph} | >50 | >50 | >50 | 39.5 ± 2.8 | 38.5 ± 4.1 | >50 | >50 | |
| NaL ^{Ph} | 29.7 ± 5.4 | 25.2 ± 2.9 | 27.5 ± 0.1 | 29.2 ± 3.4 | 28.8 ± 4.1 | >50 | >50 | |
| [Cu(L ^{Ph})(PPh ₃) ₂] | 5.1 ± 0.6 | 8.5 ± 1.5 | 6.2 ± 0.8 | 12.3 ± 2.2 | 9.8 ± 2.1 | 15.2 ± 2.8 | 25.3 ± 3.1 | |
| [Ag(L ^{Ph})(PPh ₃) ₂] | 3.0 ± 0.4 | 1.9 ± 0.8 | 3.1 ± 0.8 | 4.2 ± 1.1 | 2.4 ± 0.1 | 8.3 ± 1.9 | 9.1 ± 2.1 | |
| [Ag(L ^{Ph})(PTA)] | 35.8 ± 5.8 | 37.2 ± 2.5 | 40.7 ± 2.9 | 28.6 ± 4.1 | 25.3 ± 4.2 | >50 | >50 | |
| Cisplatin | 14.6 ± 3.0 | 13.9 ± 1.6 | 11.9 ± 1.3 | 2.1 ± 0.8 | 12.1 ± 2.8 | 9.1 ± 1.4 | 21.5 ± 4.1 | |

Cells (3-8 x 10^3 x well) were treated for 72 h with increasing concentrations of tested compounds. Cytotoxicity was assessed by MTT test. The IC₅₀ values were calculated by the four-parameter logistic model (p < 0.05).

Table 2. 3D cytotoxicity

| IC ₅₀ (μM) ± S.D. | | | | | |
|--|------------|--|--|--|--|
| | HCT-15 | | | | |
| [Cu(L ^{CF3})(PPh ₃) ₂] | 58.5 ± 5.8 | | | | |
| [Ag(L ^{CF3})(PPh ₃) ₂] | >100 | | | | |
| [Cu(L ^{Mes})(PPh ₃) ₂] | 86.6 ± 6.7 | | | | |
| [Ag(L ^{Mes})(PPh ₃) ₂] | >100 | | | | |
| [Ag(L ^{Mes})(PTA)] | >100 | | | | |
| [Cu(L ^{Ph})(PPh ₃) ₂] | >100 | | | | |
| [Ag(L ^{Ph})(PPh ₃) ₂] | 82.5 ± 5.8 | | | | |
| [Ag(L ^{Ph})(PTA)] | >100 | | | | |
| Cisplatin | 59.5 ± 3.3 | | | | |

Cells (2.5 x 10^3 x well) were treated for 72 h with increasing concentrations of tested compounds. Cytotoxicity was assessed by APH assay. The IC₅₀ values were calculated by the four-parameter logistic model (p < 0.05).

Conclusions

In this study, we report the synthesis, characterization and biological evaluation of Cu(I) and Ag(I) phosphane complexes supported by the anion of sterically hindered β-diketone ligands. In particular, 1,3-dimesitylpropane-1,3-dione (HL^{Mes}) and 1,3-bis(3,5bis(trifluoromethyl)phenyl)-3-hydroxyprop-2-en-1-one (HL^{CF3}) characterized presence of trifluoromethyl or methyl groups on the phenyl moieties were employed for the preparation of the complexes 4-11, using the lipophilic PPh3 and the hydrophilic PTA as coligands to stabilize the metal in +1 oxidation state. The analogous complexes of the anion of the parent 1,3-diphenylpropane-1,3-dione (HLPh) ligand were also synthesized and evaluated for their antitumor activity to compare the biological effects of substituents on the phenyl moieties.

The compounds were fully characterized both in solid state and in solution. X-ray crystal structures of [Cu(L^{CF3})(PPh₃)₂] and [Ag(L^{Ph})(PPh₃)₂] show that both the copper and silver complexes adopt distorted tetrahedral geometry. The diketonate based CuO₂C₃

metallacycle is essentially planar in $[Cu(L^{CF3})(PPh_3)_2]$, while the AgO_2C_3 core of $[Ag(L^{Ph})(PPh_3)_2]$ adopts a half-boat conformation with the silver atom residing out of the O_2C_3 plane.

Biological studies highlighted that both Ag(I) and Cu(I) complexes containing PPh₃ as phosphane coligand were more potent than cisplatin in inhibiting cancer cell growth. Among them, Cu complexes bearing the L^{CF3} and L^{Mes} ligands were the most effective derivatives, in particular, [Cu(L^{Mes})(PPh₃)₂] was up to 16-fold more efficacious than cisplatin in decreasing cell proliferation of 2D testis carcinoma cell cultures. Cytotoxicity experiments performed exploiting HCT-15 cell proclivity to form spheroids, showed that [Cu(L^{CF3})(PPh₃)₂] possessed a marked antiproliferative activity against 3D tumor spheroids confirming the ability of this derivative in penetrating across the entire spheroid domain and reaching the inner hypoxic core.

Experimental section

Chemistry

Materials and general methods

All the reagents were obtained from commercial sources and used as received. Melting Points (MP) were performed by an SMP3 Stuart Scientific Instrument (Bibby Sterilin Ltd., London, UK). Elemental Analyses (C, H, N) (EA) were performed with a Fisons Instruments EA-1108 CHNS-O Elemental Analyzer (Thermo Fisher Scientific Inc., Waltham, MA, USA). Fourier-Transform InfraRed (FT-IR) spectra were recorded from 4000 to 700 cm⁻¹ on a PerkinElmer Frontier Instrument (PerkinElmer Inc., Waltham, MA, USA), equipped with Attenuated Total Reflection (ATR) unit using universal diamond top-plate as sample holder. Abbreviation used in the analyses of the FT-IR spectra: br = broad, m = medium, mbr = medium broad, s = strong, sbr = strong broad, vs = very strong, w = weak, wbr = weak broad. Nuclear Magnetic Resonance (NMR) spectra for the nuclei ¹H, ¹³C and ³¹P were recorded with a Bruker 500 Ascend Spectrometer (Bruker BioSpin Corporation, Billerica, MA, USA; 500.13 MHz for ¹H, 125.78 MHz for ¹³C, 202.46 MHz for ³¹P and 470.59 MHz for ¹⁹F). Tetramethylsilane (SiMe₄) was used as external standard for the ¹H- and ¹³C-NMR spectra, while 85% H₃PO₄ was used for the ³¹P-NMR spectra. The chemical shifts (δ) are reported in ppm, and coupling constants (J) are reported in hertz (Hz). Abbreviation used in the

analyses of the NMR spectra: br = broad, d = doublet, m = multiplet, s = singlet, sbr = singlet broad, t = triplet. ElectroSpray Ionization Mass Spectra (ESI-MS) were recorded in positive-(ESI-MS(+)) or negative-ions (ESI-MS(-)) mode on a Waters Micromass ZQ Spectrometer equipped with a single quadrupole (Waters Corporation, Milford, MA, USA), using methanol or acetonitrile mobile phase. The compounds were added to reagent grade methanol or acetonitrile to give approximately 0.1 mM solutions. These solutions were injected (1 μ L) into the spectrometer fitted with an autosampler. The pump delivered the solutions to the mass spectrometer source at a flow rate of 200 μ L/min and nitrogen was employed both as a drying and nebulizing gas. Capillary voltage was typically 2500 V. The temperature of the source was 100°C, while the temperature of the desolvation was 400°C. In the analyses of ESI-MS spectra, the confirmation of major peaks was supported by comparison of the observed and predicted isotope distribution patterns, the latter calculated using the IsoPro 3.1 computer software (T-Tech Inc., Norcross, GA, USA).

NaL^{CF3} (1)

The ligand HL^{CF3} (3.000 mmol, 1.489 g) and NaOH (3.000 mmol, 0.120 g) were dissolved in ethanol (100 mL), obtaining and opalescent yellow solution. The reaction was stirred at room temperature for 4 hours. The solution was then dried at reduced pressure giving the orange solid product NaL^{CF3} in 85% yield. M.p.: 226-230 °C. FT-IR (cm⁻¹, Figure S4): 3099wbr (C-H); 1628m, 1592m (C=O); 1580sh, 1511m, 1471m, 1421m, 1360s, 1275s, 1240m, 1189m; 1163s, 1121vs (CF₃); 1044m, 955m, 905s, 887m, 845m, 787s, 702m, 681s. 1 H-NMR (DMSO-d₆, 293 K, Figure S5): δ 6.57 (s, 1H, COC*H*CO), 8.08 (s, 2H, *p*-C*H*_{ar}), 8.48 (s, 4H, *o*-C*H*_{ar}). 13 C{ 1 H}-NMR (DMSO-d₆, 293 K, Figure S6): δ 90.91 (COCHCO); 123.96 (q, 1 *J*_{CF} = 273 Hz, *C*F₃); 130.40 (q, 2 *J*_{CF} = 33 Hz, *C*CF₃); 122.88, 127.68, 146.16 (*C*H_{ar} and *C*_{ar}); 179.21 (*C*O). 19 F{ 1 H}-NMR (DMSO-d₆, 293 K, Figure S7): δ -61.21 (s). ESI-MS (major positive ions, CH₃CN), *m*/*z* (%): 541 (40) [NaL^{CF3} + Na]⁺. Elemental Analysis calculated for C₁₉H₇F₁₂NaO₂: C 44.04, H 1.36; found: C 43.89, H 1.34.

NaL^{Mes} (2)

To the ligand HL^{Mes} (2.00 mmol, 0.617 g) solubilized in methanol (15 mL), NaOH (2.000 mmol, 0.080 g) was added. The reaction mixture was stirred at reflux for 24 hours. The solution was dried at reduced pressure and the residue was recrystallized by diethyl ether and filtered. From the mother liquors, dried at reduced pressure, the light orange whitish

compound NaL^{Mes} has been obtained in 74% yield. M.p.: 102-104 °C. FT-IR (cm⁻¹, Figure S8): 3281wbr, 3147wbr, 2971wbr, 2951wbr, 2918w, 2858w (C-H); 1611m, 1565br (C=O); 1557m, 1499m, 1417sbr, 1373s, 1298w, 1271m, 1164m, 1110m, 1028mbr, 955w, 926w, 882w, 848m, 791m, 779m, 718m. 1 H-NMR (CDCl₃, 293 K, Figure S9): δ 2.23 (s, 6H, p-CH₃), 2.24 (s, 12H, o-CH₃), 5.29 (s, 1H, COCHCO), 6.72 (s, 4H, m-CH). 13 C{ 1 H}-NMR (CDCl₃, 293 K, Figure S10): δ 19.58 (o-CCH₃); 20.96 (p-CCH₃); 103.85 (COCHCO); 127.85, 132.65, 133.20, 136.10 (CH_{ar} and C_{ar}); 191.24 (CO). ESI-MS(+) (major positive ions, CH₃OH), m/z (%): 331 (100) [NaL^{Mes} + H]⁺, 353 (40) [NaL^{Mes} + Na]⁺, 683 (10) [2NaL^{Mes} + Na]⁺. ESI-MS(-) (major negative ions, CH₃OH), m/z (%): 307 (100) [L^{Mes}]⁻, 637 (10) [2L^{Mes} + Na]⁻. Elemental analysis (%) calculated for C₂₁H₂₃NaO₂: C 76.32, H 7.02; found C 74.09, H 7.09.

NaLPh (3)

The ligand HL^{Ph} (10.000 mmol, 2.243 g) and NaOH (10.000 mmol, 0.400 g) were solubilized in methanol (60 mL) and the reaction was stirred at room temperature for 24 hours under constant magnetic stirring. The precipitate formed was filtered and the mother liquors were evaporated at reduced pressure. The white product NaL^{Ph} was obtained in 80% yield. M.p.: $300\text{-}304~^{\circ}\text{C}$. FT-IR (cm⁻¹, Figure S11): 3302wbr, 3160wbr, 3058w, 2939wbr, 2827wbr; 1643w, 1596s (C=O); 1556vs, 1510s, 1452vs, 1426vs, 1383s, 1297s, 1276s, 1219s, 1176m, 1114m, 1072m, 1044s, 1012s, 999m, 946m, 937m, 851w, 814w, 785s, 767s, 730vs. $^{1}\text{H-NMR}$ (CD₃OD, 293 K, Figure S12): $^{\circ}$ 7.39-7.40 (m, 6H, $^{\circ}$ CH_{ar}), $^{\circ}$ 7.84-7.85 (m, 4H, $^{\circ}$ CH_{ar}), $^{\circ}$ 7.92-7.94 (m, 4H, $^{\circ}$ CH_{ar}). ^{1}S C{ $^{\circ}$ 1H}-NMR (acetone-d₆, 293 K, Figure S13): $^{\circ}$ 6.51 (s, 1H, COCHCO), $^{\circ}$ 7.31-7.37 (m, 6H, $^{\circ}$ CH_{ar}), $^{\circ}$ 7.92-7.94 (m, 4H, $^{\circ}$ CH_{ar}). ^{1}S C{ $^{\circ}$ 1H}-NMR (acetone-d₆, 293 K, Figure S14): $^{\circ}$ 5 91.47 (COCHCO); $^{\circ}$ 126.92, 127.69, 129.04, 143.6 (CH_{ar} and $^{\circ}$ Ca_r); 183.64 (CO). ESI-MS(+) (major positive ions, EtOH), $^{\circ}$ 7/2 (%): 247 (100) [NaL^{Ph} + H]⁺. Elemental Analysis calculated for C₁₅H₁₁NaO₂: C 73.17, H 4.50; found: C 72.51, H 4.54.

$[Cu(L^{CF3})(PPh_3)_2]$ (4)

Tetrakis(acetonitrile)copper(I) hexafluorophosphate (0.500 mmol, 0.186 g) and triphenylphosphine (1.000 mmol, 0.262 g,) were solubilized in CH₃CN (40 mL). The reaction mixture was kept under constant magnetic stirring at room temperature overnight. Then, the ligand NaL^{CF3} (0.500 mmol, 0.259 g,) was added to the solution. After 5 hours of stirring, the mixture was evaporated and the solid formed was washed in Et₂O. From the mother liquors an orange solid was precipitated, and it was crystallized using Et₂O and *n*-hexane to give

the complex **4** in 60% yield. A batch of good quality crystals of Cu(L^{CF3})(PPh₃)₂, suitable for X-ray analysis, was obtained by slow evaporation of an ethanol/acetone solution of **4**. M.p.: 109-112 °C. FT-IR (cm⁻¹, Figure S15): 3056wbr (C-H); 1626w, 1582m (C=O); 1539w, 1519w, 1501w, 1480s, 1435m, 1417m, 1360s, 1275vs, 1247m; 1171s, 1125vs (CF₃); 1097s, 1027m, 998w, 952m, 903m, 844m, 790w, 778m, 744s, 693s, 680s, 663m. ¹H-NMR (CDCl₃, 293 K, Figure S16): δ 6.17 (s, 1H, COC*H*CO), 7.22-7.41 (m, 30H, C*H*_{ar}), 7.90 (s, 2H, *p*-C*H*_{ar}), 8.11 (s, 4H, *o*-C*H*_{ar}). ¹H-NMR (DMSO-d₆, 293 K, Figure S17): δ 6.72 (s, 1H, COC*H*CO), 7.31-7.65 (m, 30H, C*H*_{ar}), 8.19 (s, 2H, *p*-C*H*_{ar}), 8.38 (s, 4H, *o*-C*H*_{ar}). ¹³C{¹H}-NMR (CDCl₃, 293 K, Figure S18): δ 92.03 (COCHCO); 123.42 (q, ¹J_{CF} = 273 Hz, CF₃); 131.23 (q, ²J_{CF} = 33 Hz, CCF₃); 123.09, 126.95, 128.43, 129.58, 133.41, 133.60, 133.79, 133.88, 144.36 (CH_{ar} and C_{ar}); 181.65 (CO). ³¹P{¹H}-NMR (CDCl₃, 223 K, Figure S19): δ -3.68 (s). ESI-MS (major positive ions, CH₃CN), *m*/*z* (%): 366 (40) [Cu(PPh₃)+ CH₃CN]+, 587 (100) [Cu(PPh₃)2]+. ¹9F{¹H}-NMR (CDCl₃, 293 K, Figure S20): δ -62.64 (s). ESI-MS (major negative ions, CH₃CN), m/*z* (%): 495 (100) [L^{CF3}]-. Elemental Analysis (%) calculated for C₅₅H₃₇CuF₁₂O₂P₂: C 60.98, H 3.44; found: C 59.95, H 3.36.

$[Ag(L^{CF3})(PPh_3)_2]$ (5)

Silver nitrate (0.500 mmol, 0.085 g,) and PPh₃ (1.000 mmol, 0.262 g) were solubilized in a methanol/acetonitrile solution (20/20 mL). The reaction mixture was stirred for 3 hours at room temperature in the dark. Subsequently, HLCF3 ligand (0.500 mmol, 0.248 g) was added and after 1 hour NaOH (0.500 mmol, 0.020 g) was added to the reaction solution. The reaction was carried on for 3 hours at room temperature in the dark. The yellow opalescent precipitate was filtered off; the solution was evaporated to dryness and the yellow solid product was solubilized in diethyl ether, purified by filtration filtered to give compound 5 in 40% yield. M.p.: 140-143 °C. FT-IR (cm⁻¹, Figure S21): 3056wbr, 2985wbr, 2855wbr (CH); 1626m, 1591m (C=O); 1524w, 1504w, 1504w, 1471m, 1456sh, 1446w, 1434m, 1425m, 1361s, 1327w, 1276vs, 1232sh, 1220m; 1168s, 1123vs (CF₃); 1095sh, 1027m, 997m, 972w, 949m. 940sh, 924m, 902m, 845m, 794m, 778m, 742s, 704sh, 692vs, 683vs. ¹H-NMR (CDCl₃, 293 K, Figure S22): δ 6.21 (s, 1H, COCHCO), 7.27-7.50 (m, 30H, CH_{ar}), 7.94 (s, 2H, p-CH_{ar}), 8.23 (s, 4H, o-CH_{ar}). ¹H-NMR (DMSO-d₆, 293 K, Figure S23): δ 6.88 (s, 1H, COCHCO), 7.37-7.50 (m, 30H, CH_{ar}), 8.23 (s, 2H, p-CH_{ar}), 8.51 (s, 4H, o-CH_{ar}). 13 C 1 H 1 -NMR (CDCl₃, 293 K, Figure S24): δ 92.35 (COCHCO); 123.38 (q, ${}^{1}J_{CF}$ = 273 Hz, CF₃); 123.42, 127.13, 128.66, 128.74, 130.08, 131.33, 132.56, 132.77, 133.91, 134.04, 144.84

(CCF₃, CH_{ar} and C_{ar}); 182.48 (CO). $^{31}P\{^{1}H\}$ -NMR (CDCl₃, 293 K, Figure S25): δ 8.88 (s). $^{31}P\{^{1}H\}$ -NMR (CDCl₃, 223 K, Figure S26): δ 8.53 (d, $^{1}J(^{107}Ag-^{31}P)$ = 430 Hz and d, $^{1}J(^{109}Ag-^{31}P)$ = 496 Hz). $^{19}F\{^{1}H\}$ -NMR (CDCl₃, 223 K, Figure S27): δ -62.66 (s). ESI-MS(+) (major positive ions, CH₃CN), m/z (%): 633 (100) [Ag(PPh₃)₂]⁺. ESI-MS(-) (major negative ions, CH₃CN), m/z (%): 495 (100) [L^{CF3}]⁻. Elemental Analysis (%) calculated for C₅₅H₃₇AgF₁₂O₂: C 58.58, H 3.31; found: C 57.61, H 3.49.

[Cu(L^{Mes})(PPh₃)₂] (**6**)

Triphenylphospine (1.000 mmol, 0.262 g) and tetrakis(acetonitrile)copper(I) hexafluorophosphate (0.500 mmol, 0.186 g) were solubilized in a mixture of CH₂Cl₂/CH₃OH (15:5 mL). The colourless clear solution was stirred at room temperature for 1 hour. Successively, the ligand NaL^{Mes} (0.500 mmol, 0.165 g) was added and the green-yellow solution was stirred at room temperature for 3 hour. The mixture was then dried at reduced pressure giving a light green solid product. The product was washed firstly in Et₂O and in a second step in CH₃OH, giving a light green precipitate that was filtered and dried under reduced pressure. The light green complex 6 was obtained in 86% yield. A batch of poor quality crystals of [Cu(LMes)(PPh3)2], suitable for X-ray analysis, was obtained by slow evaporation of an CH₂Cl₂ solution of **6**. M.p.: 210-215°C. FT-IR (cm⁻¹, Figure S28): 3050wbr, 2953wbr, 2917wbr, 2855wbr (C-H); 1613w, 1555s (C=O); 1504m, 1479m, 1434s, 1395vs, 1372s, 1311m, 1281m, 1185w, 1167m, 1113m, 1093s, 1071m, 1027m, 997m, 956w, 924w, 849s, 880m, 777m, 742s, 724m, 693vs, 608m, 541m, 525s, 503vs. ¹H-NMR (CDCl₃, 293 K, Figure S29): δ 2.13-2.34 (s, 18H, o- and p-CH₃), 5.34 (s, 1H, COCHCO), 6.74 (s, 4H, m-CH_{ar}), 7.21-7.39 (m, 30H, CH_{ar}). ¹H-NMR (DMSO-d₆, 293 K, Figure S30): δ 2.05-2.16 (s, 18H, o- and p-C H_3), 5.05 (s, 1H, COCHCO), 6.71 (s, 4H, m-C H_{ar}), 7.28-7.63 (m, 30H, C H_{ar}). ¹³C{¹H}-NMR (CDCl₃, 293 K, Figure S31): δ 19.72 (o-CCH₃); 20.96 (p-CCH₃); 103.75 (COCHCO); 127.98, 128.49, 129.36, 131.93, 132.17, 133.92, 134.04, 136.11, 141.64 (CHar and C_{ar}); 189.37 (CO). ³¹P{¹H}-NMR (CD₂Cl₂, 293 K, Figure S32): δ -5.41 (sbr). ESI-MS (+) (major positive ions, CH_2CI_2/CH_3CN) m/z (%): 587 (100) $[Cu(PPh_3)_2]^+$. ESI-MS (-) (major negative ions, CH_2CI_2/CH_3CN) m/z (%): 307 (100) [L^{Mes}]-, 341 (100) [L^{Mes} + CI]-, 396 (65) [Cu(PPh₃) + 2Cl]⁻. Elemental Analysis calculated for C₅₇H₅₃CuO₂P₂: C 76.45, H 5.97; found: C 75.97, H 5.88.

 $[Ag(L^{Mes})(PPh_3)_2]$ (7)

Silver nitrate (0.500 mmol, 0.085 g) was added to a methanol solution (20 mL) of triphenylphosphine (1.000 mmol, 0.262 g). The reaction mixture was stirred at room temperature and in the dark for one hour. Successively, the ligand NaL^{Mes} (0.500 mmol, 0.165 g) was added, and the reaction was left under constant magnetic stirring at room temperature for 4 hours. The precipitate formed was filtered and dried under reduced pressure to give the whitish complex 7 in a 40% yield. M.p.: 194-198 °C. FT-IR (cm⁻¹, Figure S33): 3054wbr, 2989wbr, 2953wbr, 2915wbr, 2851wbr (C-H); 1612w, 1582m, 1557m (C=O); 1492m, 1479m, 1435m, 1397s, 1372m, 1266m, 1182w, 1166w, 1111w, 1096s, 1071w, 1027m, 996w, 846m, 787w, 743s, 722m. ¹H-NMR (CDCl₃, 293 K, Figure S34): δ 2.22 (s, 18H, o- and p-CH₃), 5.26 (s, 1H, COCHCO), 6.73 (s, 4H, m-CH_{ar}), 7.29-7.45 (m, 30H, CH_{ar}). ¹H-NMR (DMSO-d₆, 293 K, Figure S35): δ 2.19 (s, 18H, o- and p-CH₃), 5.45 (s, 1H, COCHCO), 6.73 (s, 4H, m-CH_{ar}), 7.41-7.46 (m, 30H, CH_{ar}). ¹³C{¹H}-NMR (CDCI₃, 293 K, Figure S36): δ 19.57 (o-CCH₃); 20.98, 21.11 (p-CCH₃); 102.76 (COCHCO); 127.88, 128.46, 128.55, 128.71, 128.78, 129.87, 132.08, 132.16, 132.99, 133.18, 133.27, 133.97, 134.10, 135.67, 142.72 (CH_{ar} and C_{ar}); 190.51 (CO). $^{31}P\{^{1}H\}$ -NMR (CDCI₃, 293 K, Figure S37): δ 6.73 (s). ${}^{31}P{}^{1}H}-NMR$ (CDCl₃, 223 K, Figure S38): δ 6.22 (d, ${}^{1}J{}^{(107}Ag{}^{-31}P)$ = 408 Hz, and d, $^{1}J(^{109}Ag^{-31}P) = 472 \text{ Hz}$). ESI-MS(+) (major positive ions, CH₃OH), m/z (%): 633 (100) [Ag(PPh₃)₂]⁺. Elemental Analysis calculated for C₅₇H₅₃AgO₂P₂: C 74.84, H 5.68; found: C 73.91, H 5.62.

$[Ag(L^{Mes})(PTA)]$ (8)

To a methanol (30 mL) solution of 1,3,5-triazaphosphaadamantane (2.000 mmol, 0.314 g), AgNO₃ (1.000 mmol, 0.170 g) was added, and the solution was stirred at room temperature and in the dark for 2 hours. Successively, the ligand NaL^{Mes} was added (1,000 mmol, 0.330 g) and the reaction was left under magnetic stirring in the dark for 4 hours. The mixture was then filtered, and the precipitate was dried under reduced pressure, obtaining the orange complex 8 in 51% yield. M.p.: 193-197 °C. FT-IR (cm⁻¹, Figure S39): 3176wbr, 2948wbr, 2917wbr, 2861wbr (C-H); 1610m, 1574mbr, 1558mbr (C=O); 1497m, 1418sbr, 1373s, 1351s, 1286mbr, 1241m, 1164m, 1104m, 1039m, 1013m, 972s, 949m, 902wbr, 849m, 827mbr, 792m, 746m, 718s. ¹H-NMR (CD₃OD, 293 K, Figure S40): δ 2.24 (s, 6H, *p*-CC*H*₃), 2.32 (s, 12H, *o*-CC*H*₃), 4.28 (d, 6H, PC*H*₂N), 4.01-4.93 (m, 6H, NC*H*₂N), 6.79 (s, 4H, *m*-C*H*_{ar}).¹H-NMR (DMSO-d₆, 293 K, Figure S41): δ 2.18-2.28 (d, 18H, *p*- and *o*- CC*H*₃), 4.15

(s, 6H, PC H_2 N), 4.41-4.57 (m, 6H, NC H_2 N), 4.81 (s, 1H, COCHCO), 6.72 (s, 4H, m-C H_{ar}). 13 C{ 1 H}-NMR (DMSO-d₆, 293 K, Figure S42): δ 19.69, 21.06 (CH₃); 51.06 (PCH₂N); 72.68, 72.73 (NC H_2 N); 101.66 (COCHCO), 127.88, 132.87 (CH_{ar} and C_{ar}), 188.37 (CO). 31 P{ 1 H}-NMR (CD₃OD, 293 K, Figure S43): δ -83.73 (s). 31 P{ 1 H}-NMR (D₂O, 293 K, Figure S44): δ -81.50 (s). 31 P{ 1 H}-NMR (CD₃OD, 223 K, Figure S45): δ -81.2 (br). ESI-MS(+) (major positive ions, CH₃OH), m/z (%): 158 (100) [PTA + H]⁺, 420 (36) [Ag(PTA)₂]⁺. Elemental analysis (%) calculated for C₂₇H₃₅AgN₃O₂P: N 7.34, C 56.65, H 6.16; found: N 6.95, C 55.66, H 6.03.

$[Cu(L^{Ph})(PPh_3)_2]$ (9)

Triphenylphosphine (2.000 mmol, 0.524 g) was solubilized in CH₂Cl₂ (25 mL) and copper(I) chloride (1.000 mmol, 0.099 g) was added. The solution was stirred for 3 hours at room temperature. Successively, the ligand NaLPh (1.000 mmol, 0.246 g) was added, and the reaction was left under constant magnetic stirring for 2 hours. The mixture was filtered, and the mother liquors were evaporated at reduced pressure. The residue was washed in EtOH, filtered and dried at reduced pressure. The yellow complex 9 was obtained in 34% yield. M.p.: 209-213 °C. FT-IR (cm⁻¹, Figure S46): 3072w, 3046wbr, 3003w (C-H); 1596m, 1548s (C=O); 1511s, 1477m, 1455s, 1434s, 1403sbr, 1304m, 1273m, 1222m, 1179m, 1160m, 1092m, 1068m, 1022m, 997m, 936m, 922mbr, 840w, 806w, 784m, 741s, 719s. ¹H-NMR (CDCl₃, 293 K, Figure S47): δ 6.40 (s, 1H, COCHCO), 7.24-7.44 (m, 36H, CH_{ar}), 7.79 (d, 4H, CH_{ar}). ¹H-NMR (DMSO-d₆, 293 K, Figure S48): δ 6.47 (s, 1H, COCHCO), 7.29-7.42 (m, 36H, CH_{ar}), 7.83 (d, 4H, CH_{ar}). ¹³ $C\{^{1}H\}$ -NMR (CDCl₃, 293 K, Figure S49): δ 93.06 (COCHCO); 126.91, 127.80, 128.35, 128.42, 128.46, 128.55, 129.32, 132.08, 132.16, 133.93, 134.05, 134.14 (CH_{ar} and C_{ar}); 184.59 (CO). ³¹P{¹H}-NMR (CDCl₃, 293 K, Figure S50): δ -3.96 (s). ESI-MS(+) (major positive ions, CH₃CN), m/z (%): 587 (100) $[(L^{Ph})Cu(PPh_3) + K]^+$. ESI-MS(-) (major negative ions, CH₃CN), m/z (%): 223 (100) $[L^{Ph}]^-$. Elemental Analysis calculated for C₅₁H₄₁CuO₂P₂: C 75.50, H 5.09; found: C 74.11, H 4.62.

$[Ag(L^{Ph})(PPh_3)_2]$ (10)

Triphenylphosphine (2.000 mmol, 0.524 g) was solubilized in methanol (50 mL) and AgNO₃ (1.000 mmol, 0.170 g) was added. The reaction was stirred in the dark for 2 hours. Successively, the ligand NaL^{Ph} (1.000 mmol, 0.246 g) and the mixture was left under constant magnetic stirring in the dark for 4 hours. The solution was then filtered, and the precipitate was dried under reduced pressure to give the yellow-orange complex **10** in 54%

yield. A batch of good quality crystals of [Ag(LPh)(PPh3)2], suitable for X-ray analysis, was obtained by slow evaporation of a chloroform/hexane solution of **10**. M.p.: 193-197 °C. FT-IR (cm-1, Figure S51): 3071mbr, 3045mbr, 3004br (CH); 1598m, 1557m (C=O); 1505s, 1477m, 1453s, 1434s, 1407sbr, 1333m, 1300m, 1258m, 1216m, 1178m, 1160m, 1093m, 1066m, 1026m, 1019m, 966m, 933m, 933m, 921m, 912m, 841m, 780m, 737s, 720s, 705s. 1 H-NMR (CDCl3, 293 K, Figure S52): δ 6.41 (s, 1H, COC*H*CO), 7.29-7.40 (m, 23H, C*H*_{ar}), 7.46-7.50 (m, 13H, C*H*_{ar}), 7.85 (t, 4H, C*H*_{ar}). 1 H-NMR (DMSO-d₆, 293 K, Figure S53): δ 6.41 (s, 1H, COC*H*CO), 7.34-7.38 (m, 23H, C*H*_{ar}), 7.39-7.47 (m, 13H, C*H*_{ar}), 7.84 (t, 4H, C*H*_{ar}). 1 3C{ 1 H}-NMR (CDCl3, 293 K, Figure S54): δ 93.38 (COCHCO); 127.02, 127.18, 127.78, 128.45, 128.55, 128.69, 128.71, 132.08, 132.16, 133.93, 134.05, 134.14 (*C*H_{ar} and *C*_{ar}); 186.02 (CO). 3 1P{ 1 H}-NMR (CDCl3, 293 K, Figure S55): δ 7.24 (s). 3 1P{ 1 H}-NMR (CDCl3, 293 K, Figure S56): δ 7.21 (dbr, 1 J(Ag- 3 P) = 439 Hz). ESI-MS(+) (major positive ions, CH3CN), m/z (%): 633 (100) [Ag(PPh3)2] $^{+}$. Elemental Analysis calculated for C₅₁H₄₁AgO₂P₂: C 71.59, H 4.89; found: C 71.14, H 4.58.

$[Ag(L^{Ph})(PTA)] \cdot H_2O(11)$

The 1,3,4-triazaphosphaadamantane (2.000 mmol, 0.314 g) was solubilized in methanol (30 mL) and AgNO₃ (1.000 mmol, 0.170 g) was added. The reaction was stirred in the dark at room temperature for 2 hours. Successively, the ligand NaLPh (1.000 mmol, 0.246 g) was added and the solution was stirred in the dark at room temperature for 4 hours. The mixture was then filtered and the precipitate was dried under reduced pressure. The orange product was recovered to give complex 11 in 81% yield. M.p.: 198-203 °C. FT-IR (cm⁻¹, Figure S57): 3225mbr (O-H); 3060mbr, 2942mbr (C-H); 1598s, 1555s (C=O); 1513s, 1466s, 1419vs, 1345vsbr, 1289vs, 1242s, 1225s, 1180mbr, 1102s, 1069m, 1039m, 1013s, 971vs, 947vs, 898s, 843m, 828m, 804m, 790m, 745vs, 712vs. ¹H-NMR (CD₃OD, 293 K, Figure S58): δ 4.25 (d, 6H, PCH₂N), 4.56-4.67 (m, 6H, NCH₂N), 4.86 (H₂O), 6.78 (br, 1H, COCHCO), 7.48 (s, 5H, CH_{ar}), 7.95 (s, 5H, CH_{ar}). ¹H-NMR (D₂O, 293 K, Figure S59): δ 4.08 (d, 6H, PCH_2N), 4.45-4.51 (m, 6H, NCH₂N), 6.32 (s, 1H, COCHCO), 7.42-7.43 (s, 5H, CH_{ar}), 7.73 (s, 5H, C H_{ar}). ¹H-NMR (DMSO, 293 K, Figure S60): δ 4.13 (d, 6H, PC H_2 N), 4.39-4.55 (m, 6H, NCH_2N), 6.45 (s, 1H, COCHCO), 7.42 (s, 5H, CH_{ar}), 7.90 (s, 5H, CH_{ar}). ¹³C{¹H}-NMR (CD₃OD, 293 K, Figure S61): 50.10 (PCH₂N); 72.00, 72.05 (NCH₂N); 90.35 (COCHCO); 126.76, 127.28, 128.07, 128.29, 128.36, 128.84 (CH_{ar} and C_{ar}), 179.93 (CO). ³¹P{¹H}-NMR (CD₃OD, 293 K, Figure S62): δ -83.82 (s). ³¹P{¹H}-NMR (CD₃OD, 223 K, Figure S63): δ - 81.5 (br). ESI-MS(+) (major positive ions, CH₃OH), m/z (%): 158 (100) [PTA + H]⁺, 421 (8) [Ag(PTA)₂]⁺. Elemental Analysis (%) calculated for C₂₁H₂₅AgN₃O₃P: N 8.30, C 49.82, H 4.98; found: N 8.95, C 48.93, H 4.88.

X-ray Structure Determinations

A suitable crystal covered with a layer of hydrocarbon/Paratone-N oil was selected and mounted on a Cryo-loop, and immediately placed in the low temperature nitrogen stream. The X-ray intensity data of HLCF3 and [Cu(LCF3)(PPh3)2] were measured at 100 K on a SMART APEX II CCD area detector system while X-ray intensity data of [Ag(LPh)(PPh3)2] were measured at 100(2) K on a Bruker D8 Quest equipped with a PHOTON II 7 CPAD detector. These systems were equipped with an Oxford Cryosystems 700 series cooler, a graphite monochromator, and a Mo K α fine-focus sealed tube ($\lambda = 0.71073$ Å). Intensity data were processed using the Bruker Apex program suite. Absorption corrections were applied by using SADABS. 115 Initial atomic positions were located by SHELXT, 116 and the structures of the compounds were refined by the least-squares method using SHELXL¹¹⁷ within Olex2 GUI. 118 All the non-hydrogen atoms were refined anisotropically. Hydrogen atoms were included at calculated positions and refined using appropriate riding models. The molecule HLCF3 sites on a twofold rotation axis and the O-H position is therefore disordered over two oxygen sites. [Cu(LCF3)(PPh3)2] crystallizes in P-1 space group with two chemically similar molecules in the asymmetric unit. X-ray structural figures were generated using Olex2. CCDC 2279297-2279299 files contain the supplementary crystallographic data. These data be obtained free of charge via can http://www.ccdc.cam.ac.uk/conts/retrieving.html or from the Cambridge Crystallographic Data Centre (CCDC), 12 Union Road, Cambridge, CB2 1EZ, UK). Additional details are provided in supporting information section. We have also collected single crystal X-ray data on [Cu(L^{Mes})(PPh₃)₂] and obtained its molecular structure. Unfortunately, the crystal quality is poor and suffers also due to twinning. As a result, the structure is not of sufficient quality for detailed analysis of metrical parameters. The atom connectivity and basic features of the molecule are however clear from the data (see Supporting Information, Tables S1-S9).

Experiments with Cultured Human Cancer Cells

Ag(I) and Cu(I) complexes and the corresponding uncoordinated ligands and related salts were dissolved in DMSO just before the experiment, and a calculated amount of drug

solution was added to the cell growth medium to a final solvent concentration of 0.5%, which had no detectable effects on cell viability. Cisplatin was dissolved in 0.9% sodium chloride solution. MTT (3-(4,5-dimethylthiazol-2-yl)-2,5-diphenyltetrazolium bromide) and cisplatin were obtained from Sigma Chemical Co, St. Louis, MO, USA.

Cell Cultures

Human SCLC (U1285), NSCLC (A549), testis (NTERA-2), colon (HCT-15), and pancreatic (PSN-1 and BxPC3) carcinoma cell lines were obtained by American Type Culture Collection (ATCC, Rockville, MD, USA). Cell lines were maintained in the logarithmic phase at 37 °C in a 5% carbon dioxide atmosphere using RPMI-1640 medium (EuroClone, Milan, Italy) containing 10% fetal calf serum (EuroClone, Milan, Italy), antibiotics (50 units/mL penicillin and 50 µg/mL streptomycin) and 2 mM I-glutamine.

MTT Assay

The growth inhibitory effect toward tumor cells was evaluated by means of MTT assay as previously described.⁸⁵ IC₅₀ values, the drug concentrations that reduce the mean absorbance at 570 nm to 50% of those in the untreated control wells, were calculated by the four-parameter logistic (4-PL) model. Evaluation was based on means from at least three independent experiments.

Spheroid Cultures and Acid Phosphatase (APH) Assay

Spheroid cultures were obtained by seeding 2.5x10³ HCT-15 human cancer cells/well in a round-bottom non-treated tissue culture 96-well plate (Greiner Bio-one, Kremsmünster, Austria) in phenol red free RPMI-1640 medium (Sigma Chemical Co., St. Louis, MO, USA) containing 10% fetal calf serum and supplemented with 20% methyl cellulose stock solution. An APH modified assay was employed for evaluating cell viability in 3D spheroids, as previously described.⁸⁵ IC₅₀ values (drug concentrations that reduce the mean absorbance at 405 nm 50% of those in the untreated control wells) were calculated by 4-PL model. Evaluation was based on means from at least three independent experiments.

Supporting Information

The Supporting Information is available free of charge at https://pubs.acs.org/doi...

Accession Codes

CCDC 2279297-2279299 contain the supplementary crystallographic data for this paper. These data can be obtained free of charge via www.ccdc.cam.ac.uk/data_request/cif, or by emailing data_request@ccdc.cam.ac.uk, or by contacting The Cambridge Crystallographic Data Centre, 12 Union Road, Cambridge CB2 1EZ, UK; fax: +44 1223 336033.

Conflict of interest

The authors declare no competing financial interests.

Acknowledgments

This work was supported by Unione Europea – NextGenerationEU (MUR-Fondo Promozione e Sviluppo - D.M. 737/2021, INVIRCuM, University of Camerino, FAR 2022 PNR, and NGEU PNRR, D.M. n. 351/2022 M4C1 I4.1) and by the University of Padova (PRID BIRD225980). H.V.R.D. acknowledges the support by the National Science Foundation through grant CHE-1954456.

References

- 1. K. D. Mjos and C. Orvig, *Chem. Rev.*, 2014, **114**, 4540-4563.
- 2. N. P. E. Barry and P. J. Sadler, *Chem. Commun.*, 2013, **49**, 5106-5131.
- 3. A. Casini, A. Vessières and S. M. Meier-Menches, eds., *Metal-based Anticancer Agents*, The Royal Society of Chemistry, Croydon (UK), 2019.
- 4. A. Sigel, E. Freisinger and R. K. O. Sigel, eds., *Metallo-Drugs: Development and Action of Anticancer Agents*, De Gruyter, 2018.
- 5. S. Medici, M. Peana, V. M. Nurchi and M. A. Zoroddu, *J. Med. Chem.*, 2019, **62**, 5923-5943.
- 6. C. Santini, M. Pellei, V. Gandin, M. Porchia, F. Tisato and C. Marzano, *Chem. Rev.*, 2014, **114**, 815-862.
- 7. S. Nobili, E. Mini, I. Landini, C. Gabbiani, A. Casini and L. Messori, *Med. Res. Rev.*, 2010, **30**, 550-580.
- 8. J. A. Joule and K. Mills, *Heterocyclic Chemistry*, Wiley, Chichester (UK), Fifth edn., 2010.
- 9. C. Y. Chen, J. C. Lien, C. Y. Chen, C. C. Hung and H. C. Lin, *Int. J. Mol. Sci.*, 2021, **22**, 12171.
- 10. C. Pettinari, F. Marchetti and A. Drozdov, in *Compr. Coord. Chem. II*, eds. J. A. McCleverty and T. J. Meyer, Pergamon, Oxford, 2003, pp. 97-115.
- 11. A. R. Siedle, in *Compr. Coord. Chem.*, eds. G. Wilkinson, R. D. Gillard and J. A. McCleverty, Pergamon, Oxford, UK, 1987, pp. 365-412.
- 12. A. S. Crossman and M. P. Marshak, in *Compr. Coord. Chem. III*, eds. E. C. Constable, G. Parkin and L. Que Jr, Elsevier, Oxford, 2021, pp. 331-365.
- 13. M. Stalpaert and D. De Vos, *ACS Sustainable Chem. Eng.*, 2018, **6**, 12197-12204.

- 14. A. S. Crossman, A. T. Larson, J. X. Shi, S. M. Krajewski, E. S. Akturk and M. P. Marshak, *J. Org. Chem.*, 2019, **84**, 7434-7442.
- 15. S. M. Krajewski, A. S. Crossman, E. S. Akturk, T. Suhrbier, S. J. Scappaticci, M. W. Staab and M. P. Marshak, *Dalton Trans.*, 2019, **48**, 10714-10722.
- 16. E. S. Akturk, S. J. Scappaticci, R. N. Seals and M. P. Marshak, *Inorg. Chem.*, 2017, **56**, 11466-11469.
- 17. T. Schilling, K. B. Keppler, M. E. Heim, G. Niebch, H. Dietzfelbinger, J. Rastetter and A. R. Hanauske, *Invest. New Drugs*, 1995, **13**, 327-332.
- 18. H. Bischoff, M. R. Berger, B. K. Keppler and D. Schmähl, *J. Cancer Res. Clin. Oncol.*, 1987, 113, 446-450.
- 19. A. Wu, D. C. Kennedy, B. O. Patrick and B. R. James, *Inorg. Chem. Commun.*, 2003, **6**, 996-1000.
- 20. R. Fernández, M. Melchart, A. Habtemariam, S. Parsons and P. J. Sadler, *Chem. Eur. J.*, 2004, **10**, 5173-5179.
- 21. M. Melchart, A. Habtemariam, S. Parsons and P. J. Sadler, *J. Inorg. Biochem.*, 2007, **101**, 1903-1912.
- 22. C. A. Vock, A. K. Renfrew, R. Scopelliti, L. Juillerat-Jeanneret and P. J. Dyson, *Eur. J. Inorg. Chem.*, 2008, 1661-1671.
- 23. C. Aliende, M. Pérez-Manrique, F. A. Jalón, B. R. Manzano, A. M. Rodríguez, J. V. Cuevas, G. Espino, M. Á. Martínez, A. Massaguer, M. González-Bártulos, R. De Llorens and V. Moreno, *J. Inorg. Biochem.*, 2012, **117**, 171-188.
- 24. S. Seršen, J. Kljun, K. Kryeziu, R. Panchuk, B. Alte, W. Körner, P. Heffeter, W. Berger and I. Turel, *J. Med. Chem.*, 2015, **58**, 3984-3996.
- 25. J. Kljun and I. Turel, *Eur. J. Inorg. Chem.*, 2017, **2017**, 1655-1666.
- 26. J. Conradie and J. C. Swarts, *Dalton Trans.*, 2011, **40**, 5844-5851.
- 27. J. Conradie and J. C. Swarts, Eur. J. Inorg. Chem., 2011, 2011, 2439-2449.
- 28. J. Do Couto Almeida, I. M. Marzano, F. C. S. De Paula, M. Pivatto, N. P. Lopes, P. C. De Souza, F. R. Pavan, A. L. B. Formiga, E. C. Pereira-Maia and W. Guerra, *J. Mol. Struct.*, 2014, **1075**, 370-376.
- 29. D. I. Ugwu and J. Conradie, *J. Inorg. Biochem.*, 2023, 112268.
- 30. A. Muscella, N. Calabriso, C. Vetrugno, F. P. Fanizzi, S. A. De Pascali, C. Storelli and S. Marsigliante, *Biochem. Pharmacol.*, 2011, **81**, 91-103.
- 31. A. Muscella, N. Calabriso, C. Vetrugno, F. P. Fanizzi, S. A. De Pascali and S. Marsigliante, *Biochem. Pharmacol.*, 2011, **81**, 1271-1285.
- 32. A. Muscella, N. Calabriso, C. Vetrugno, L. Urso, F. P. Fanizzi, S. A. De Pascali and S. Marsigliante, *Br. J. Pharmacol.*, 2010, **160**, 1362-1377.
- 33. A. Muscella, N. Calabriso, F. P. Fanizzi, S. A. De Pascali, L. Urso, A. Ciccarese, D. Migoni and S. Marsigliante, *Br. J. Pharmacol.*, 2008, **153**, 34-49.
- 34. K. Nakano, T. Nakayachi, E. Yasumoto, S. R. Morshed, K. Hashimoto, H. Kikuchi, H. Nishikawa, K. Sugiyama, O. Amano, M. Kawase and H. Sakagami, *Anticancer Res.*, 2004, **24**, 711-717.
- 35. J. J. Wilson and S. J. Lippard, *J. Med. Chem.*, 2012, **55**, 5326-5336.
- 36. S. A. Gromilov and I. A. Baidina, *J. Struct. Chem.*, 2004, **45**, 1031-1081.
- 37. L. G. Bulusheva, A. V. Okotrub, T. I. Liskovskaya, S. A. Krupoder, A. V. Guselnikov, A. V. Manaev and V. F. Traven, *J. Phys. Chem. A*, 2001, **105**, 8200-8205.
- 38. K. M. Chi, H. K. Shin, M. J. Hampden-Smith, E. N. Duesler and T. T. Kodas, *Polyhedron*, 1991, **10**, 2293-2299.
- 39. A. T. Larson, A. S. Crossman, S. M. Krajewski and M. P. Marshak, *Inorg. Chem.*, 2020, **59**, 423-432.
- 40. H. Lang, M. Leschke, M. Melter, B. Walfort, K. Kohler, S. E. Schulz and T. Gessner, *Z. Anorg. Allg. Chem.*, 2003, **629**, 2371-2380.
- 41. H. K. Shin, K. M. Chi, J. Farkas, M. J. Hampden-Smith, T. T. Kodas and E. N. Duesler, *Inorg. Chem.*, 1992, **31**, 424-431.
- 42. K.-M. Chi, J. Farkas, M. J. Hampden-Smith, T. T. Kodas and E. N. Duesler, *Dalton Trans.*, 1992, 3111-3117.

- 43. H. K. Shin, M. J. Hampden-Smith, E. N. Duesler and T. T. Kodas, *Can. J. Chem.*, 1992, **70**, 2954-2966.
- 44. T. H. Baum and C. E. Larson, *Chem. Mater.*, 1992, **4**, 365-369.
- 45. S. K. Reynolds, C. J. Smart, E. F. Baran, T. H. Baum, C. E. Larson and P. Brock, *J. Appl. Phys. Lett.*, 1991, **59**, 2332.
- 46. D. B. Beach, F. K. LeGoues and C. K. Hu, *Chem. Mater.*, 1990, **2**, 216-219.
- 47. Y. L. Chow and G. E. Buono-Core, *Can. J. Chem.*, 1983, **61**, 795-800.
- 48. R. J. Restivo, A. Costin, G. Ferguson and A. J. Carty, *Can. J. Chem.*, 1975, **53**, 1949-1957.
- 49. W. A. Anderson, A. J. Carty, G. J. Palenik and G. Schreiber, *Can. J. Chem.*, 1971, **49**, 761-766.
- 50. A. Jakob, C. C. Joubert, T. Rüffer, J. C. Swarts and H. Lang, *Inorg. Chim. Acta*, 2014, **411**, 48-55.
- 51. P. Tasker, A. Parkin, T. C. Higgs, S. Parsons and D. Messanger, *CSD Communication* (*Private Communication*), 2005.
- 52. R.-N. Yang, D.-M. Wang, Y.-F. Liu and D.-M. Jin, *Polyhedron*, 2001, **20**, 585-590.
- 53. S. A. Gulyaev, E. S. Vikulova, T. S. Sukhikh, I. Y. Ilyin and N. B. Morozova, *J. Struct. Chem.*, 2021, **62**, 1836-1845.
- 54. I. S. Fedoseev, E. S. Vikulova, I. Y. Il'in, A. I. Smolentsev, M. R. Gallyamov and N. B. Morozova, *J. Struct. Chem.*, 2016, **57**, 1667-1670.
- 55. K. Akhbari and A. Morsali, *Cryst. Growth Des.*, 2007, **7**, 2024-2030.
- 56. W. J. Evans, D. G. Giarikos, D. Josell and J. W. Ziller, *Inorg. Chem.*, 2003, **42**, 8255-8261.
- 57. C. Y. Xu, T. S. Corbitt, M. J. Hampdensmith, T. T. Kodas and E. N. Duesler, *Dalton Trans.*, 1994, 2841-2849.
- 58. E. S. Vikulova, T. S. Sukhikh, S. A. Gulyaev, I. Y. Ilyin and N. B. Morozova, *Molecules*, 2022, **27**. 677.
- 59. F. Marandi, M. Ghadermazi, A. Marandi, I. Pantenburg and G. Meyer, *J. Mol. Struct.*, 2011, **1006**, 136-141.
- 60. A. J. Blake, N. R. Champness, S. M. Howdle, K. S. Morley, P. B. Webb and C. Wilson, *CrystEngComm*, 2002, **4**, 88-92.
- 61. Y. L. Shen, J. L. Jin, G. X. Duan, P. Y. Yu, Y. P. Xie and X. Lu, *Chem. Eur. J.*, 2021, **27**, 1122-1126.
- 62. J. L. Jin, Y. P. Xie, H. Cui, G. X. Duan, X. Lu and T. C. W. Mak, *Inorg. Chem.*, 2017, **56**, 10412-10417.
- 63. H. Liu, S. Battiato, A. L. Pellegrino, P. Paoli, P. Rossi, C. Jimenez, G. Malandrino and D. Munoz-Rojas, *Dalton Trans.*, 2017, **46**, 10986-10995.
- 64. A. O. Rybaltovskii, V. G. Arakcheev, A. N. Bekin, A. F. Danilyuk, V. I. Gerasimova, N. V. Minaev, E. N. Golubeva, O. O. Parenago and V. N. Bagratashvili, *Russ. J. Phys. Chem. B*, 2015, **9**, 1137-1142.
- 65. G. Calabrese, S. Petralia, D. Franco, G. Nocito, C. Fabbi, L. Forte, S. Guglielmino, S. Squarzoni, F. Traina and S. Conoci, *Mater. Sci. Eng., C*, 2021, **118**, 111394.
- 66. H. Schmidt, A. Jakob, T. Haase, K. Kohse-Hoinghaus, S. E. Schulz, T. Wachtler, T. Gessner and H. Lang, *Z. Anorg. Allg. Chem.*, 2005, **631**, 2786-2791.
- 67. D. A. Edwards, R. M. Harker, M. F. Mahon and K. C. Molloy, *J. Mater. Chem.*, 1999, **9**, 1771-1780.
- 68. Z. Yuan, N. H. Dryden, J. J. Vittal and R. J. Puddephatt, *Chem. Mater.*, 1995, **7**, 1696-1702.
- 69. Z. Yuan, N. H. Dryden, J. J. Vittal and R. J. Puddephatt, *Can. J. Chem.*, 1994, **72**, 1605-1609
- 70. N. H. Dryden, J. J. Vittal and R. J. Puddephatt, *Chem. Mater.*, 1993, **5**, 765-766.
- 71. W. Lin, T. H. Warren, R. G. Nuzzo and G. S. Girolami, *J. Am. Chem. Soc.*, 1993, **115**, 11644-11645.
- 72. S. Wanninger, V. Lorenz, A. Subhan and F. T. Edelmann, *Chem. Soc. Rev.*, 2015, **44**, 4986-5002.
- 73. M. H. M. Leung, T. Harada and T. W. Kee, *Curr. Pharm. Des.*, 2013, **19**, 2070-2083.

- 74. Y. Figueroa-DePaz, K. Resendiz-Acevedo, S. G. Dávila-Manzanilla, J. C. García-Ramos, L. Ortiz-Frade, J. Serment-Guerrero and L. Ruiz-Azuara, *J. Inorg. Biochem.*, 2022, **231**, 111772.
- 75. J. Serment-Guerrero, M. E. Bravo-Gomez, E. Lara-Rivera and L. Ruiz-Azuara, *J. Inorg. Biochem.*, 2017, **166**, 68-75.
- 76. I. Correia, S. Borovic, I. Cavaco, C. P. Matos, S. Roy, H. M. Santos, L. Fernandes, J. L. Capelo, L. Ruiz-Azuara and J. C. Pessoa, *J. Inorg. Biochem.*, 2017, **175**, 284-297.
- 77. L. Ruiz-Azuara and M. E. Bravo-Gomez, *Curr. Med. Chem.*, 2010, **17**, 3606-3615.
- 78. L. Polloni, A. C. D. Silva, S. C. Teixeira, F. V. D. Azevedo, M. A. P. Zoia, M. S. da Silva, P. Lima, L. I. V. Correia, J. D. Almeida, C. V. da Silva, V. D. R. Avila, L. R. F. Goulart, S. Morelli, W. Guerra and R. J. de Oliveira, *Biomed. Pharmacother.*, 2019, **112**, 108586.
- 79. D. A. Paixao, B. C. A. de Oliveira, J. D. Almeida, L. M. Sousa, C. D. Lopes, Z. A. Carneiro, D. Y. Tezuka, J. C. T. Clavijo, J. Ellena, L. Polloni, P. H. A. Machado, S. de Albuquerque, R. J. de Oliveira, S. Guilardi and W. Guerra, *Inorg. Chim. Acta*, 2020, **499**, 119164.
- 80. R. E. Malekshah, M. Salehi, M. Kubicki and A. Khaleghian, *J. Coord. Chem.*, 2019, **72**, 1697-1714.
- 81. R. E. Malekshah, M. Salehi, M. Kubicki and A. Khaleghian, *J. Coord. Chem.*, 2018, **71**, 952-968
- 82. A. Pramanik, D. Laha, P. Pramanik and P. Karmakar, J. Drug Targeting, 2014, 22, 23-33.
- 83. D. F. Xu, Z. H. Shen, Y. Shi, Q. He and Q. C. Xia, *Russ. J. Coord. Chem.*, 2010, **36**, 458-462
- 84. L. A. Khamidullina, I. S. Puzyrev, G. L. Burygin, P. V. Dorovatovskii, Y. V. Zubavichus, A. V. Mitrofanova, V. N. Khrustalev, T. V. Timofeeva, P. A. Slepukhin, P. D. Tobysheva, A. V. Pestov, E. Solari, A. G. Tskhovrebov and V. G. Nenajdenko, *Molecules*, 2021, **26**, 6466.
- 85. M. Pellei, C. Santini, L. Bagnarelli, M. Caviglia, P. Sgarbossa, M. De Franco, M. Zancato, C. Marzano and V. Gandin, *Int. J. Mol. Sci.*, 2023, **24**, 4091.
- 86. F. Del Bello, M. Pellei, L. Bagnarelli, C. Santini, G. Giorgioni, A. Piergentili, W. Quaglia, C. Battocchio, G. Iucci, I. Schiesaro, C. Meneghini, I. Venditti, N. Ramanan, M. De Franco, P. Sgarbossa, C. Marzano and V. Gandin, *Inorg. Chem.*, 2022, **61**, 4919-4937.
- 87. M. Pellei, L. Bagnarelli, L. Luciani, F. Del Bello, G. Giorgioni, A. Piergentili, W. Quaglia, M. De Franco, V. Gandin, C. Marzano and C. Santini, *Int. J. Mol. Sci.*, 2020, **21**, 2616.
- 88. M. B. Morelli, C. Amantini, G. Santoni, M. Pellei, C. Santini, C. Cimarelli, E. Marcantoni, M. Petrini, F. Del Bello, G. Giorgioni, A. Piergentili and W. Quaglia, *New J. Chem.*, 2018, **42**, 11878-11887.
- 89. V. Gandin, C. Ceresa, G. Esposito, S. Indraccolo, M. Porchia, F. Tisato, C. Santini, M. Pellei and C. Marzano, *Sci. Rep.*, 2017, **7**, 13936.
- 90. F. Tisato, C. Marzano, V. Peruzzo, M. Tegoni, M. Giorgetti, M. Damjanovic, A. Trapananti, A. Bagno, C. Santini, M. Pellei, M. Porchia and V. Gandin, *J. Inorg. Biochem.*, 2016, **165**, 80-91.
- 91. G. Papini, G. Bandoli, A. Dolmella, G. Gioia Lobbia, M. Pellei and C. Santini, *Inorg. Chem. Commun.*, 2008, **11**, 1103-1106.
- 92. M. Inoue, Y. Sumii and N. Shibata, ACS Omega, 2020, **5**, 10633-10640.
- 93. E. P. Gillis, K. J. Eastman, M. D. Hill, D. J. Donnelly and N. A. Meanwell, *J. Med. Chem.*, 2015, **58**, 8315-8359.
- 94. S. Purser, P. R. Moore, S. Swallow and V. Gouverneur, *Chem. Soc. Rev.*, 2008, **37**, 320-330.
- 95. P. Shah and A. D. Westwell, *J. Enzyme Inhib. Med. Chem.*, 2007, **22**, 527-540.
- 96. L. H. Doerrer and H. V. R. Dias, *Dalton Trans.*, 2023, **52**, 7770-7771.
- 97. S. Swallow, in *Prog. Med. Chem.*, eds. G. Lawton and D. R. Witty, Elsevier, 2015, vol. 54, pp. 65-133.
- 98. I. M. Abdou, A. M. Saleh and H. F. Zohdi, *Molecules*, 2004, **9**, 109-116.
- 99. P. N. Edwards, in *Organofluorine Chemistry: Principles and Commercial Applications*, eds. R. E. Banks, B. E. Smart and J. C. Tatlow, Springer US, Boston, MA, 1994, pp. 501-541.
- 100. C. R. Groom, I. J. Bruno, M. P. Lightfoot and S. C. Ward, *Acta Crystallogr., Sect. B: Struct. Sci., Cryst. Eng. Mater.*, 2016, **B72**, 171-179.

- 101. J. S. Lakhi, M. R. Patterson and H. V. R. Dias, New J. Chem., 2020, 44, 14814-14822.
- 102. C. Zhang, P. Yang, Y. Yang, X. Huang, X.-J. Yang and B. Wu, *Synth. Commun.*, 2008, **38**, 2349-2356.
- 103. J. Emsley, in *Complex Chemistry. Structure and Bonding*, eds. J. Emsley, R. D. Ernst, B. J. Hathaway and K. D. Warren, Springer, Berlin, Heidelberg, 1984, vol. 57, pp. 147-191.
- 104. M. A. Halcrow, J.-S. Sun, J. C. Huffman and G. Christou, *Inorg. Chem.*, 1995, **34**, 4167-4177.
- 105. R. P. Dryden and A. Winston, *J. Phys. Chem.*, 1958, **62**, 635-637.
- 106. B. Cheng, H. Yi, C. He, C. Liu and A. Lei, *Organometallics*, 2014, **34**, 206-211.
- 107. C. He, G. Zhang, J. Ke, H. Zhang, J. T. Miller, A. J. Kropf and A. Lei, *J. Am. Chem. Soc.*, 2013, **135**, 488-493.
- 108. S. N. Slabzhennikov, O. B. Ryabchenko and L. A. Kuarton, *Russ. J. Coord. Chem.*, 2006, **32**, 545-551.
- 109. A. Guerriero, M. Peruzzini and L. Gonsalvi, Coord. Chem. Rev., 2018, 355, 328-361.
- 110. A. M. Kirillov, S. W. Wieczorek, M. F. C. Guedes da Silva, J. Sokolnicki, P. Smoleński and A. J. L. Pombeiro, *CrystEngComm*, 2011, **13**, 6329-6333.
- 111. H. V. R. Dias, J. A. Flores, M. Pellei, B. Morresi, G. Gioia Lobbia, S. Singh, Y. Kobayashi, M. Yousufuddin and C. Santini, *Dalton Trans.*, 2011, **40**, 8569-8580.
- 112. M. Pellei, S. Alidori, G. Papini, G. Gioia Lobbia, J. D. Gorden, H. V. R. Dias and C. Santini, *Dalton Trans.*, 2007, 4845-4853.
- 113. H. V. R. Dias, S. Alidori, G. Gioia Lobbia, G. Papini, M. Pellei and C. Santini, *Inorg. Chem.*, 2007, **46**, 9708-9714.
- 114. S. El Harane, B. Zidi, N. El Harane, K.-H. Krause, T. Matthes and O. Preynat-Seauve, *Journal*, 2023, **12**, 1001.
- 115. L. Krause, R. Herbst-Irmer, G. M. Sheldrick and D. Stalke, J. Appl. Cryst., 2015, 48, 3-10.
- 116. G. M. Sheldrick, Acta Crystallogr. Sect. A: Found. Adv., 2015, A71, 3-8.
- 117. G. M. Sheldrick, Acta Crystallogr. Sect. C: Struct. Chem., 2015, C71, 3-8.
- 118. O. V. Dolomanov, L. J. Bourhis, R. J. Gildea, J. A. K. Howard and H. Puschmann, *J. Appl. Crystallogr.*, 2009, **42**, 339-341.